$K\alpha$, $K\beta$, and radiative Auger photon intensities in K x-ray spectra from atoms in the $20 \leq Z \leq 40$ region

J. L. Campbell, A. Perujo, W. J. Teesdale, and B. M. Millman
Guelph Waterloo Program for Graduate Work in Physics, University of Guelph, Guelph, Ontario, Canada N1G 2W1
(Received 25 September 1985)

Accurate measurements of the x-ray intensity ratio $I(K\beta)/I(K\alpha)$ from electron-capture radionuclides, using Si(Li) detectors of calibrated line shape, eliminate an existing large discrepancy between experiment and relativistic Hartree-Fock predictions. Small systematic discrepancies in the literature ratios for the mechanisms of photoionization, and electron and proton excitation, are attributed to omission of radiative Auger (RA) satellites in spectrum analysis. With the inclusion of RA peaks in the spectrum fitting, the present data support Scofield's predictions of $I(K\beta)/I(K\alpha)$ at the 1% accuracy level, an important conclusion for elemental analysis techniques such as proton-induced x-ray emission and x-ray fluorescence. The resulting radiative Auger intensities also agree quite well with calculations.

I. INTRODUCTION

The x-ray intensity ratio $I(K\beta)/I(K\alpha)$ has been extensively studied in recent years. It is the ratio of the radiative transition probabilities when a K vacancy is filled from the $M,N,O,\ldots$ shells to that for filling from the L shell, and is thus a gross ratio involving several transitions. Prior to 1974 a systematic discrepancy[1] emerged across the entire Periodic Table between $I(K\beta)/I(K\alpha)$ ratios measured by Si(Li) and Ge(Li) spectrometers and the predictions of Scofield's relativistic Hartree-Slater (RHS) calculations.[2] This appeared to be resolved by Scofield's relativistic Hartree-Fock (RHF) calculations[3] which took proper account of overlap and exchange effects.

However, a compilation of measured values by Berényi *et al.*[4] suggests that at $Z < 40$ the trend of experimental data actually falls between the RHS and RHF predictions.

The work reported in this paper is the first to employ an accurately measured detector resolution function (obtained using monoenergetic photons) and the first to consider explicitly the radiative Auger satellites, which are important at low atomic numbers. It is, therefore, potentially much more accurate than previous studies. The importance of having accurate values of $I(K\beta)/I(K\alpha)$ in applications such as PIXE and XRF provided another reason for the work.

Any study of $I(K\beta)/I(K\alpha)$ ratios must take into consideration recent reports of dependence both upon the ionization mechanism and the chemical environment of the emitting atoms. A brief review of these is necessary before the present work is described.

II. PERTURBATIONS OF THE RATIO $I(K\beta)/I(K\alpha)$

Berényi *et al.*[4] observed that values of $I(K\beta)/I(K\alpha)$ measured by Si(Li) and Ge(Li) spectroscopy using electron-capture (EC) radionuclides tend to be lower than those obtained by proton, photon, or electron bombardment.

Early investigations,[5-7] centering on Cr, Mn, and Fe demonstrated significant variations of $I(K\beta)/I(K\alpha)$ with chemical environment but the range of results was less in photo-ionization ($\sim 6\%$) than electron capture ($\sim 18\%$). These early studies disagreed as to the existence of a correlation between $I(K\beta)/I(K\alpha)$ and the emitting atom's valence state. Collins *et al.*[8] expressed concern about the adequacy of matrix corrections in Refs. 5 and 6, and measured $I(K\beta)/I(K\alpha)$ for thin ^{51}Cr-containing samples using a Si(Li) spectrometer. Their results, 0.1316 for Cr, 0.1382 for Cr III, and 0.1467 for Cr VI finally confirmed a strong correlation of $I(K\beta)/I(K\alpha)$ with oxidation number of the initial Cr atom.

Turning now to mechanisms we have first the early comparison of $I(K\beta)/I(K\alpha)$ in EC and PI by Paić and Pečar.[9] This suggested that $I(K\beta)/I(K\alpha)$ in electron capture at a given Z was less than the corresponding value of the ratio in photoionization (PI); the difference was about 10% at $Z=22$, but fell steadily with increasing Z, disappearing at $Z \sim 30$. However, little detail of chemical purity or matrix corrections was given and much of the observed effect could simply be due to chemical environment. Moreover, a comparison between PI and EC is not well defined since the atoms involved cannot exist in identical chemical environments. Brunner *et al.*[10] therefore made a more definitive comparison between photon (PI) and proton (PIXE) ionization in the $20 < Z < 40$ region. They found variations of up to 5% with chemical environment with essentially the same behavior in PI and PIXE.

Clearly then chemical variations are twice as large in EC as in PI and PIXE (there is no electron work), and in EC the effect correlates strongly with valence. Possibly $I(K\beta)/I(K\alpha)$ is slightly less in the EC case. Arndt *et al.*[11] predict the latter observation by viewing the x-ray emitting EC daughter as retaining the parent atom's electron configuration and hence having one excess $3d$ electron; this reduces the $1s$-$3p$ orbital overlap and hence the $K\beta$ intensity. As regards chemical variations, varying $3d$-charge delocalization should have similar effects whatever the mechanism[8,10] upon the $1s$-$3p$ overlap simply by

changing the screening of the $3p$ electrons. Brunner *et al.*[10] performed transition rate calculations that took these effects into account and explained most, though not all, of the $\sim 5\%$ effects seen in PI and PIXE.

This leaves one to explain the greater chemical effects in EC and to this end Brunner[12] examined the effect of nuclear recoil; this deforms the electron cloud, causing additional valence-$1s$ transitions which enhance the ratio $I(K\beta)/I(K\alpha)$ and render it more sensitive to valence state. However, such an enhancement of $I(K\beta)/I(K\alpha)$ is at variance with Berényi's observation[4] that $I(K\beta)/I(K\alpha)$ values from EC tend to be lower than those from PI or PIXE, although the increased chemical sensitivity does agree with observation. For this reason precise measurements of $I(K\beta)/I(K\alpha)$ for the EC case were the main aim of the present work.

III. PREVIOUS $K\beta/K\alpha$ MEASUREMENTS

In this section we discuss reported work based on Si(Li), Ge, and Ge(Li) spectroscopy. We have chosen to omit the relatively small input from wavelength-dispersive spectroscopy because of the assumptions it has to make concerning crystal reflectivity.

The 1974 review by Salem *et al.*[1] concluded that measured ratios $I(K\beta)/I(K\alpha)$ agreed with Scofield's RHF predictions at the $\pm 2\%$ level. By 1978 the quantity of available data was much greater, especially in the case of proton excitation. In their review Berényi *et al.* were able to discern a general trend for experimental values to fall a little below the RHF theory, this effect being more pronounced at lower Z values and especially clear in the case of the electron-capture mechanism. In 1980, Khan and Karimi[13] collected 216 ratios obtained by various mechanisms and covering the entire Periodic Table. They fitted polynomials to these data in the regions $Z \leq 20$, $20 \leq Z \leq 30$, and $Z \geq 30$. There is excellent agreement between the fitted curves and the RHF values except in two regions; in the range $20 \leq Z \leq 30$ the fit falls clearly below the theory and this must be taken seriously in view of the plethora of data here; above $Z = 80$, where data become sparse, there is a tendency for the fit again to fall low.

Our interest here is in the $20 \leq Z \leq 40$ region because of the observed discrepancy and because of chemical influences. We have therefore extracted all the data in this region from Refs. 4 and 13, and added some further results by Heinrich *et al.*[14] and Collins *et al.*[8] (photon ionization and electron excitation). We have undoubtedly omitted some existing measurements, but those used are quite sufficient to buttress the arguments made here.

In the case of photon, electron, and proton excitation we use only data from elemental targets. For EC all the data are perforce from chemical compounds dried from solution to provide thin sources on thin backings. Figure 1(a) presents the mean ratio $I(K\beta)/I(K\alpha)$ for each element as a function of mechanism (excluding EC). We have not used an error-weighted mean; the errors quoted are partly subjective, and within a given excitation technique we expect the true uncertainties to be similar provided detector resolution if reasonably good (which means values of 140—200 eV for the full width at half maximum of a 5.9 keV peak) and counting statistics are adequate. (Of course differing backgrounds will result in different errors in one excitation method relative to another.) Table I presents the ratio of theoretical to mean experimental values and indicates the number of experimental data points utilized. Electron data by Mistry and Quarles[15] were omitted due to their divergence from the four other electron data sets.

Figure 1(a) and Table I show up a well-defined trend. In the Ti-Ni region of the $3d$ transition elements, experiment is systematically below theory; the effect grows with decreasing Z, reaching 3% at Ti. The point $Z = 24$ is anomalous; Table I suggests that here experiment and theory agree; however, Fig. 1(b) shows that the theory dips here (solid circle) while the data are consistent with

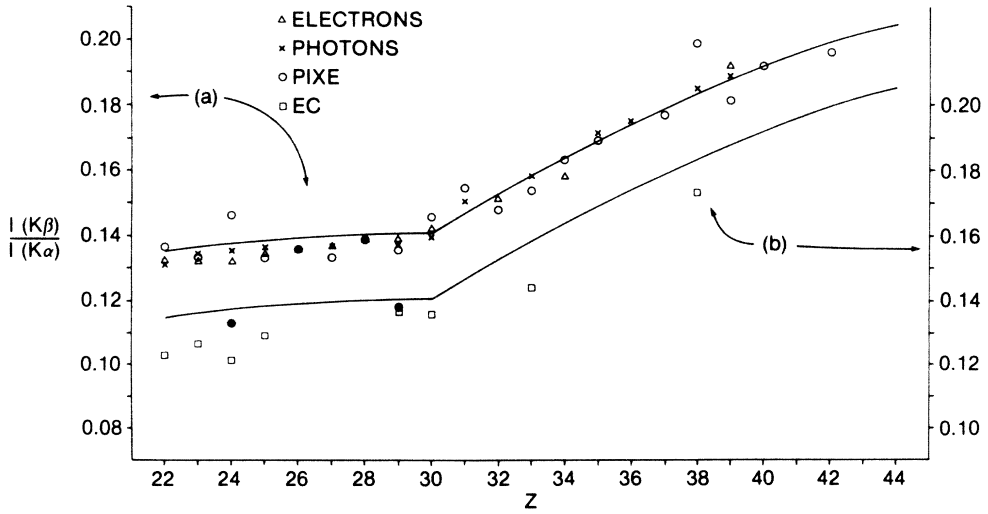

FIG. 1. Ratio of theoretical $I(K\beta)/I(K\alpha)$ (Ref. 3) to mean experimental values from the literature. (a) K vacancies created by photoionization, electron, and proton bombardment. (b) K vacancies created by nuclear electron capture. The solid circles in (b) are anomalous theoretical points at $Z = 24$ and 29.

TABLE I. Ratio of Scofield's RHF predictions of $I(K\beta)/I(K\alpha)$ to mean experimental results.

	Ionization mechanism		
Z	Photons	Electrons	Protons
22	1.032(4)	1.027(3)	0.995(2)
23	1.020(2)	1.036(2)	1.019(2)
24	0.994(3)	1.008(2)	0.921(1)
25	1.018(1)	1.027(2)	1.039(1)
26	1.027(4)	1.027(2)	1.024(4)
27	1.015(1)	1.024(3)	1.052(3)
28	1.014(2)	1.005(3)	1.008(3)
29	1.0015(3)	0.986(4)	1.020(5)
30	1.011(2)	0.988(3)	0.968(1)
32	1.003(2)	0.987(1)	1.018(1)
33			1.017(1)
34	1.027(2)	1.023(2)	1.002(1)
35			0.993(1)
36	1.007(1)		
37	1.018(1)		1.0085(2
38			0.919(1)
39	1.012(2)	0.973(2)	1.030(1)
40	1.019(1)		0.998(1)

the overall trend. Obviously the theoretical datum at $Z=24$ is anomalous with respect to the other theoretical points in this region, as has been discussed already by Salem *et al.*[16] and by Khan and Karim.[13] A similar but lesser effect occurs at $Z=29$ [solid circle in Fig. 1(b)].

Figure 1(b) reveals much greater and nonsystematic disagreement in the EC case.[8,9,17] Experiment is markedly less than theory although chemical effects and neutrino recoil effects would result in the opposite behavior[12], i.e., an increase in $I(K\beta)/I(K\alpha)$ over the elemental value.

IV. RADIATIVE AUGER SATELLITES

An alternative deexcitation mode for a K vacancy is the simultaneous emission of a bound electron and an x-ray photon. This results in the $K\beta$ line having a low-energy (KMM) satellite, corresponding to a K-M photon transition with ejection of an M electron; similarly the $K\alpha$ line has satellites designed KLL and KLM. Aberg[18,19] showed that the line strength for the RA process vanishes if the participating electrons are assumed to be in frozen orbitals; hence the existence of RA satellites in K x-ray spectra is a clear indication of the need to incorporate in the theory the relaxation of orbitals between the initial and final states; this is done in Scofield's RHF work.[4]

The limited experimental work on the RA satellites has almost all been done by traditional crystal-diffr ion spectroscopy. Recent work on KMM satellites in the transition metal spectra,[20,21] despite uncertainties of 50—100% gives satellite relative intensities that agree quite well with Scofield's predictions.

None of the experimental work cited in Secs. II and III mentions the RA process in analyzing the data. The gross K-$L_{2,3}$ and K-$M_{2,3},N_{2,3}$ photon lines in Si(Li) spectra are generally designated as $K\alpha$ and $K\beta$, and their intensity ratio compared specifically with Scofield's tabulated relative transition probabilities (RTP) $I(K\beta)/I(K\alpha)$. However, in this tabulation, Scofield includes KMM in the $K\beta$ probability, and $KLL+KLM$ in the $K\alpha$ probability. In the experimental spectra these three RA satellites fall largely within the low-energy tails usually imputed to incomplete charge collection, and do not give rise to resolved peaks.

In the present experimental work we follow Scofield by including RA satellites in our measurement of the relative $K\alpha$ and $K\beta$ transition probabilities. We use the term $I(K\beta)/I(K\alpha)^*$ to designate the RTP of the single-vacancy transitions K-$M_{2,3},N_{2,3}$ and K-$L_{2,3}$.

At $Z=24$, Scofield predicts $I(KLM)/I(K\alpha)\simeq 0.5\%$ and $I(KMM)/I(K\beta)\simeq 4.8\%$. If these contributions are ignored in fitting the spectra (say by using one Gaussian for the K-$L_{2,3}$ photon line and one for the K-$M_{2,3},N_{2,3}$ photon line), then a 4.3% underestimate of $I(K\beta)/I(K\alpha)$ will result. If the peak tails are imputed to incomplete charge collection and the observed $K\alpha$ tail used as a model for the $K\beta$ tail (as has often been the case) there will still be an underestimate. This level of underestimate is close to that observed for PI, PIXE, and electron bombardment in Fig. 1(a); hence the systematic discrepancy may be due to experimenter's neglect of the RA process. As Z increases beyond 30, the RA contributions diminish rapidly; here there is no systematic discrepancy.

In the EC case between $Z=20$ and $Z=30$, the RA effect is not sufficient to explain the discrepancies. Here there are far fewer experimental data than for the other three mechanisms.

V. OBJECTIVES OF THE PRESENT WORK

The aim here is to measure $I(K\beta)/I(K\alpha)$ for EC sources, where the discrepancies appear to be much greater than can be explained by neglect of the radiative Auger process. This is done with Si(Li) detectors whose line shape has been accurately determined as a function of energy using monoenergetic photons. By fitting the EC x-ray spectra with the known resolution function, first excluding and then including the radiative Auger satellites we can demonstrate that the latter are indeed a source of systematic error at the level observed in Fig. 1 and Table I.

VI. EXPERIMENTAL DETAIL

Thin EC sources of ^{51}Cr, ^{54}Mn, ^{55}Fe, ^{57}Co, ^{65}Zn, and ^{75}Se were made by evaporation of chlorides *in vacuo* from a heated tantalum filament onto a masked beryllium disk of 0.05 mm thickness. The spot deposits were 2.5 mm in diameter. The evaporation temperature of about 800 °C would provide only partial dissociation of some of the chlorides, hence we expect varying mixtures of the valence states I and II in our sources, with II predominating.

The K x-ray spectra were recorded using two different Si(Li) detectors. Detector A had thickness 3.3 mm, nominal area 80 mm^2 and energy resolution 185 eV at 6.4 keV; the corresponding figures for detector B were 30 mm^2, 5.0 mm, and 170 eV. Tantalum and aluminum apertures of 4

mm diameter were used to restrict photons to the central portion of each detector. The pulse-height analysis system was a Nuclear Data model 66 equipped with a ND575 analog-to-digital converter and a ND595 digital spectrum stabilizer. The total intensities in spectra taken with detector A were $(1-2)\times10^6$. However, $(5-7)\times10^6$ counts were recorded in each spectrum taken with the higher resolution detector B, and in this case a pile-up rejector was included in the electronic system. Counting rates were held below 500 s^{-1}.

The line shape was determined for each detector as a function of energy, using an x-ray generator equipped with a curved crystal monochromator. Use of a range of anodes allowed us to select $K\alpha_1$, $K\beta_1$, and $L\alpha_1$ lines in the range 2–25 keV. In each case the energy "bandpass" was about 5 eV. Since this is, to our knowledge, the first such study of a Si(Li) detector, it is described in detail elsewhere[22] and so there is no need to duplicate the description here.

It was found that between 5 and 15 keV the function

$$F(i)=G(i)+S(i)+D(i)$$

where

$$G(i)=H_G\exp\left[-\frac{(i-i_0)^2}{2\sigma^2}\right],$$

$$S(i)=\tfrac{1}{2}H_S\,\mathrm{erfc}\left[\frac{i-i_0}{\sigma\sqrt{2}}\right], \qquad (1)$$

$$D(i)=\tfrac{1}{2}H_D\exp\left[\frac{i-i_0}{\beta}\right]\mathrm{erfc}\left[\frac{i-i_0}{\sigma\sqrt{2}}+\frac{\sigma}{\beta\sqrt{2}}\right],$$

TABLE II. Reduced χ_r^2 values for fits of Eq. (1) to line shapes produced by monoenergetic photons. Each line had 10^6 counts intensity.

Line	Energy (keV)	Reduced χ_r^2 Detector A[a]	Detector B[b]
Sc $K\alpha_1$	4.0906	2.84	1.05
Cr $K\alpha_1$	5.415	1.83	1.06
Fe $K\alpha_1$	6.404	0.96	1.24
Fe $K\beta_1$	7.06	1.13	
Cu $K\alpha_1$	8.048	1.01	1.17
Cu $K\beta_1$	8.90	1.00	
Ge $K\alpha_1$	9.886	0.93	1.10
Ge $K\beta_1$	10.98	1.26	1.48
Zr $K\alpha_2$	15.691	1.27	1.22

[a]Fitted with one long-term tail.
[b]Fitted with a long-term and a short-term tail.

provided excellent fits to the peaks from detector A. Table II shows the reduced χ_r^2 values for detector A in the 5–15 keV range normalized to peak intensity 10^6 counts. Figure 2 shows the fit for this detector for the iron $K\alpha_1$ line at 6.404 keV. The parameters H_D, H_S, and β, which characterize the peak imperfections varied smoothly with energy, as shown for the H_D case in Fig. 3.

All the fitting was done with a conventional, nonlinear least-squares technique on a Digital Equipment Corporation MINC 11/23 computer.

The fits of Eq. (1) to the spectra from detector B were poorer, and to attain similar quality a second (short-term) tail had to be added. This catered for a slight peak asym-

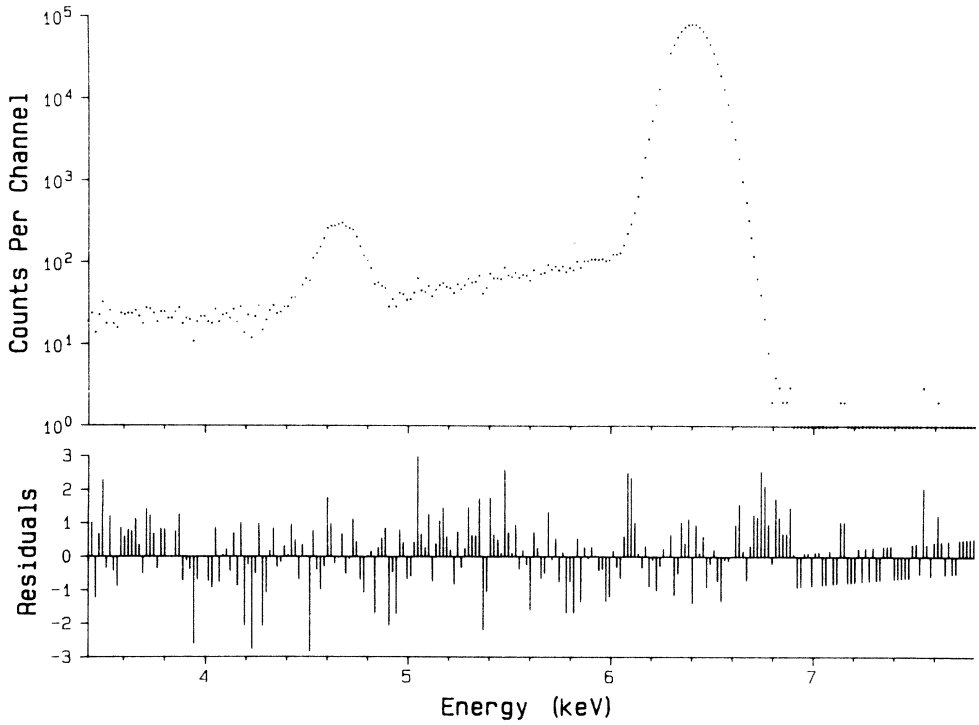

FIG. 2. Response of detector A to monoenergetic radiation of energy 6.404 keV.

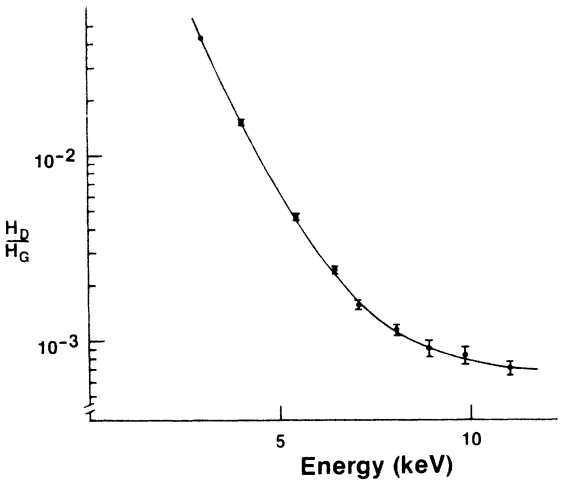

FIG. 3. Energy dependence of the line shape parameter H_D/H_G for detector A.

metry revealed by the superior resolution of this detector.

The thickness of the silicon deadlayer on each detector was deduced from the energy dependence of the relative area of $D(i)$ as described in Ref. 22. The beryllium-window thickness was determined by attenuation measurements on duplicate window foils using a highly collimated ^{55}Fe source of 25 mCi activity. The window-to-crystal distance for each detector was determined[23] with the same source using the inverse-square law. The thickness of the gold electrode was obtained from the intensity of the gold $L\alpha$ x-ray peak fluoresced by monochromatized Zr $K\alpha_2$ photons. The crystal thickness was determined from the measured curve of absolute efficiency versus energy, which was obtained using calibrated radionuclide x-ray sources;[23] the thickness was taken as a variable in a least-squares fit of the expression describing absolute efficiency[24] to our measured data points. The values for detectors A and B were 3.3 and 4.7 mm, respectively.

This careful characterization of the detectors provided the basis for a reliable interpretation of the K x-ray spectra from EC radionuclides. These spectra were first fitted with two Hypermet peaks representing the two main x-ray lines, plus three Gaussians representing KLL, KLM, and KMM; the Si escape peaks were included according to the intensity prescription of Johansson,[35] which we have tested rigorously elsewhere.[22] Gaussian representation of KLM and KMM is justified since the detector resolution is much larger than the spread of individual KL_iM_j and KM_iM_j lines within each RA band; it neglects the tail to low energy, but since wavelength-dispersive studies[20,21]

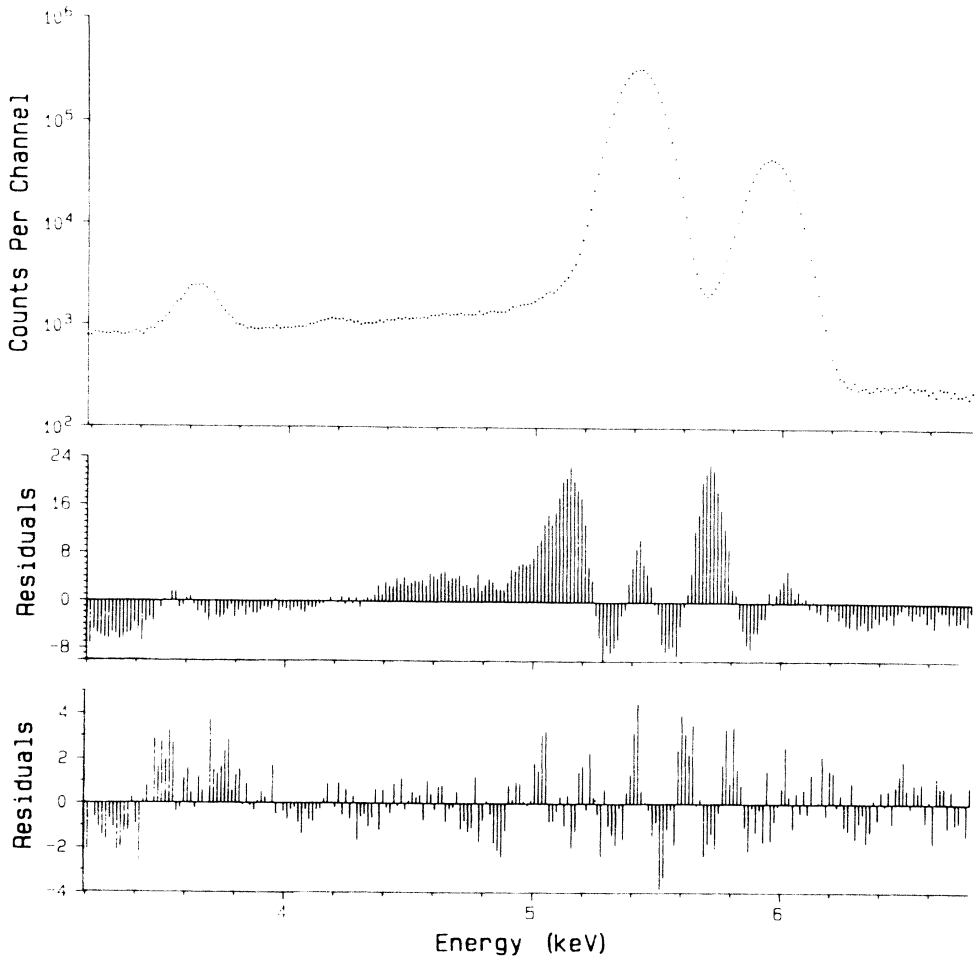

FIG. 4. Details of the fit to a chromium K x-ray spectrum from ^{54}Mn decay using detector B. The upper residue corresponds to a fit which ignored the RA satellites; the lower residue resulted from their inclusion in the model.

show that most of the RA intensity is within two FWHM's of the RA maximum energy, this is justifiable.

The centroids X_0 and widths σ of the various peaks of energy E_k were given by

$$(X_0)_k = a_1 + a_2 E_k \ , \qquad \sigma_k^2 = a_3 + a_4 E_k \ , \tag{2}$$

where $a_1, \ldots, a_4$ were variables of the fit. The tail and shelf parameters for the two major peaks were interpolated from the monoenergetic photon results and held fixed in the fits. The heights of the various lines were allowed to vary. Since the energies of *KLM* and *KMM* lines were not known *a priori* these were also variables.

The *KLL* band is much broader than *KLM* or *KMM*. We found it impossible to achieve a good fit with a single Gaussian whose width was dictated by Eq. (2). A combination of two Gaussians, their energies adjusted empirically, served reasonably well.

Figure 4 shows the results of fits to the K x-ray spectrum of chromium obtained with detector B; the data and the residuals (data minus fit in units of one standard deviation) are displayed. When the RA satellites were omitted from the model, the residual spectrum exhibited peaks in the *KLL*, *KLM*, and *KMM* energy regions. Inclusion of the satellites in the model led to uniform residues. The reduced χ_r^2 values for these fits, normalized to 10^6 counts intensity, are in Table III.

Finally, in the ^{75}Se case, the $K\alpha_1$-$K\alpha_2$ and $K\beta_1$-$K\beta_2$ separations were too large for us to use single peaks for each of $K\alpha$ and $K\beta$. Instead, two Hypermet peaks were used to represent $K\alpha$ and two to represent $K\beta$; the $I(K\alpha_2)/I(K\alpha_1)$ and $I(K\beta_3)/I(K\beta_1)$ ratios held at Scofield's theoretical values, and the $K\alpha_1$ and $K\beta_1$ heights were fitted.

VII. DISCUSSION OF RESULTS

Table IV presents the measured values of $I(K\beta)/I(K\alpha)^*$ together with Scofield's predictions; any disagreements are at the 1—2% level as opposed to the 10% effect reported in previous work [see Fig. 1(b)]. This result is reinforced by a visual comparison of our $I(K\beta)/I(K\alpha)$ with Scofield's curve[3] in Fig. 5. Clearly the present work has brought the EC data much closer to theory than before. If any residual discrepancy persists here, it is on the side of excessive experimental values at $Z=23,24,25$ and at a level of 1—2% that is consistent with chemical effects. The valence state of II prevailing for most of our sources caused a 3% increase over the elemental result in the work of Collins *et al.*[8] on chromium. Our results for Cr are consistent with this.

Figures 6 and 7 separate out the radiative Auger results for $I(KMM)/(K\beta)$ and $I(KLM)/I(K\alpha)$. We did not regard our $I(KLL)/I(K\alpha)$ results as quantitatively useful, despite the clear indication of the *KLL* process in Fig. 4.

Neither set of *KMM* data agrees well with Scofield's theoretical values.[4] However, the data taken with detector B, which had markedly better energy resolution, agree quite well with wavelength-dispersive data;[20,21] both the latter tend to follow the calculated value for 3*s*- and 3*p*-electron ejection; this appears acceptable since *KMM* events involving 3*d* electrons are probably integrated into the main $K\beta$-photon peak.

Our *KLM* results scatter widely but their mean trend follows the theory rather well. The scatter is to be expected; we are extracting from the $K\alpha$ peak a satellite of

TABLE III. Reduced χ_r^2 values for fits to K x-ray spectra from EC radionuclides; the values are normalized to a constant spectral intensity of 10^6 counts.

Element	Z	Radionuclide	χ_r^2 Detector A	χ_r^2 Detector B
V	23	^{51}Cr	1.775	1.19
Cr	24	^{54}Mn	1.32	1.22
Mn	25	^{55}Fe		1.49
Fe	26	^{57}Co	2.38	1.56
Cu	29	^{65}Zn	2.44	1.33
As	33	^{75}Se	2.94	3.74

TABLE IV. Measured relative transition probability $I(K\beta)/I(K\alpha)^*$ for M,N-K and L-K single-vacancy transitions.

Z	Detector A	Detector B	Theory (Ref. 3)
23	0.1330[b]	0.1371	0.1318
24	0.1334	0.1358	0.1329[a]
25		0.1369	0.1339
26	0.1312	0.1367	0.1343
29	0.1371	0.1364	0.1363[a]
33	0.1533	0.1526	0.1517

[a]Since Scofield's (Ref. 3) values at $Z=24,29$ do not follow the trend established for other elements, these two values are interpolated.

[b]Experimental uncertainties are estimated at ±1%.

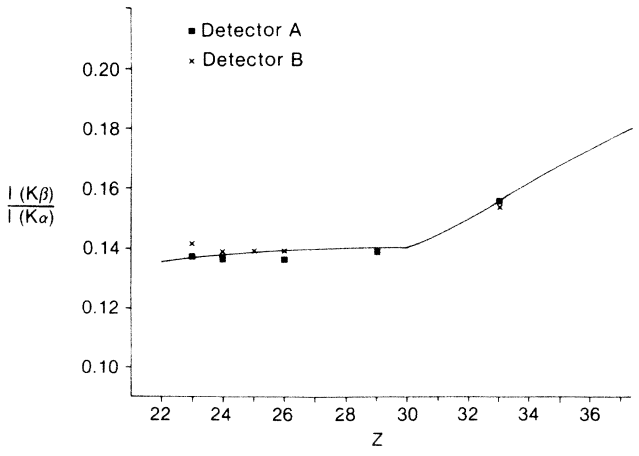

FIG. 5. Present results for $I(K\beta)/I(K\alpha)$ compared with RHF calculation (curve). Uncertainties are estimated at ±1%.

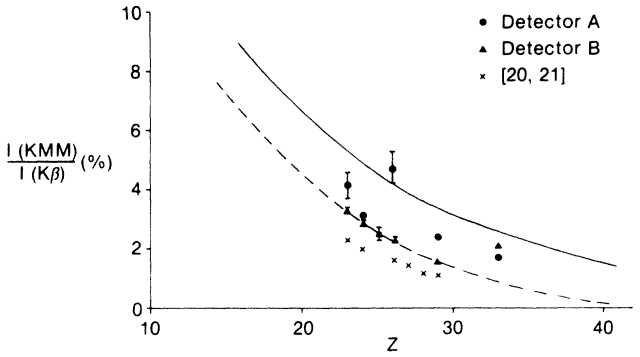

FIG. 6. Measured relative transition probabilities $I(KMM)/I(K\beta)$ compared with theory (Ref. 3). The solid line is the basic theoretical value and the dashed line that for RA transitions involving $3s$ and $3p$ ejection only (Refs. 20 and 21). Typical 1σ error bars are shown.

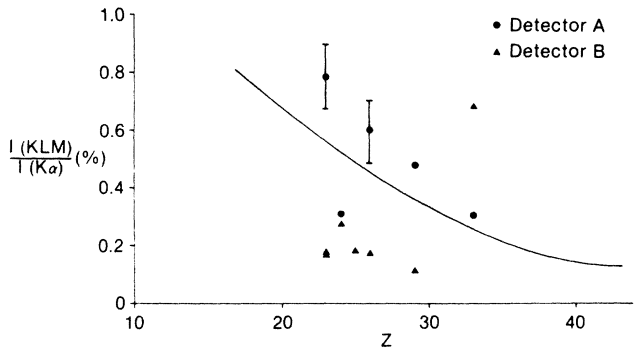

FIG. 7. Measured relative transition probabilities $I(KLM)/I(K\alpha)$ compared with theory (Ref. 3).

$\sim 0.5\%$ intensity which sits in a low-energy tail of very similar intensity. Figure 7 shows the typical error given by the fitting program, but given these intensities, we feel that a $\pm 25\%$ error on our mean values would be realistic.

VIII. CONCLUSIONS

We have argued that the existing data base of relative transition probabilities $I(K\beta)/I(K\alpha)$ measured using PI, PIXE, or electron bombardment differs from theory in the $20 \leq Z \leq 30$ region only because experimenters have ignored radiative Auger satellites. Inclusion of RA peaks in the present experimental study based on EC source results in $I(K\beta)/I(K\alpha)$ ratios that agree with RHF predictions in the 1–2 % level. There may be a slight upward shift in $I(K\beta)/I(K\alpha)$ due to the existence of a valence-state mixture of Cr and Cr II.

These conclusions should provide a firmer basis for new work on chemical perturbations of the $I(K\beta)/I(K\alpha)$ ratio, whatever the ionization mechanism, than has existed hitherto. It is likely that the radiative Auger process itself will be strongly influenced by chemical bonding.

The agreement of our EC results with theory suggests that neutrino recoil effects on $I(K\beta)/I(K\alpha)$ are small. This does not preclude an enhanced sensitivity to chemical bonding caused by these effects. Since chemical bonding has been shown[5,6,8] to increase $I(K\beta)/I(K\alpha)$, the low EC results of Hansen *et al.*[17] and of Paić and Pečar[9] must have some other cause, probably of an experimental nature.

Our $I(KMM)/I(K\beta)$ ratios agree with previous wavelength-dispersive work, both data sets suggesting that the RA satellite observed corresponds to $3s$- and $3p$-electron ejection. The only other Si(Li) study is a very recent one by Marageter *et al.*,[26] who do not discuss the intrinsic detector line shape in detail; their data scatter widely above and below the theory. Our $I(KLM)/I(K\alpha)$ ratios are the only ones measured by Si(Li) spectroscopy, and we merely note that within a wide scatter, they tend to follow the theory. The agreement with theory to within a factor 2 or better for this 0.5% effect should serve to buttress confidence in the results for $I(K\beta)/I(K\alpha)$ which are the main focus of this work.

Finally, the present indications that theoretical $I(K\beta)/I(K\alpha)$ values are correct to within 1% for proton, photon, and electron bombardment lends confidence to the use of these values as a data base in elemental analysis techniques based upon characteristic x-ray emission.

ACKNOWLEDGMENT

This work is supported by the Natural Sciences and Engineering Research Council of Canada.

[1]S. I. Salem, S. L. Panossian, and R. A. Krause, At. Data Nucl. Data Tables **14**, 91 (1974).
[2]J. H. Scofield, Phys. Rev. **179**, 9 (1969).
[3]J. H. Scofield, Phys. Rev. A **9**, 1041 (1974).
[4]D. Berényi, G. Hock, S. Ricz, B. Schlenk, and A. Valek, J. Phys. B **11**, 709 (1978).
[5]A. L. F. Lazzarini, E. Lazzarini, and M. M. Bettoni, Radiochim. Acta **25**, 81 (1978).
[6]Y. Tanaki, T. Omori, and T. Shiokawa, Radiochem. Radioanal. Lett. **37**, 39 (1979).
[7]B. Paci-Mazzilli and D. S. Urch in *Inner-Shell and X-Ray Physics of Atoms and Solids*, edited by D. J. Fabian, H. Kleinpoppen, and L. M. Watson (Plenum, New York, 1981), p. 741.
[8]K. E. Collins, C. H. Collins, and C. Heitz, Radiochim. Acta **28**, 7 (1981).
[9]G. Paić and V. Pečar, Phys. Rev. A **14**, 2190 (1976).

[10]G. Brunner, M. Nagel, E. Hartmann, and E. Arndt, J. Phys. B **15**, 4517 (1982).
[11]E. Arndt, G. Brunner, and E. Hartmann, J. Phys. B **15**, L887 (1982).
[12]G. Brunner, J. Phys. B **16**, 1199 (1983).
[13]Md. R. Khan and M. Karimi, X-Ray Spectrom. **9**, 32 (1980).
[14]K. F. J. Heinrich, C. E. Fiori, and R. L. Myklebust, J. Appl. Phys. **50**, 5589 (1979).
[15]V. D. Mistry and C. A. Quarles, Nucl. Phys. **A164**, 219 (1971).
[16]S. I. Salem, T. H. Falconer, and R. E. Winchell, Phys. Rev. A **6**, 2147 (1972).
[17]J. S. Hansen, H.-U. Freund, and R. W. Fink, Nucl. Phys. **A153**, 465 (1970).
[18]T. Aberg, Phys. Rev. A **4**, 1735 (1971).
[19]T. Aberg in *Atomic Inner-Shell Processes,* edited by B. Crasemann (Academic, New York, 1975), p. 353.
[20]A. Servomaa and O. Keski-Rahkonen, J. Phys. C **8**, 4124 (1975).
[21]O. Keski-Rakhonen and J. Ahopelto, J. Phys. C **13**, 471 (1980).
[22]J. L. Campbell, B. M. Millman, J. A. Maxwell, A. Perujo, and W. J. Teesdale, Nucl. Instrum. Methods B **9**, 71 (1985).
[23]J. L. Campbell, R. G. Leigh, and W. J. Teesdale, Nucl. Instrum. Methods B **5**, 39 (1984).
[24]D. D. Cohen, Nucl. Instrum. Methods **178**, 481 (1980).
[25]G. I. Johansson, X-Ray Spectrom. **11**, 194 (1982).
[26]E. Margeter, W. Wegscheider, and K. Müller, X-Ray Spectrom. **13**, 78 (1984).